

# Effects of non-thermal tails in Maxwellian electron distributions on synchrotron and Compton processes

Grzegorz Wardziński<sup>\*</sup> and Andrzej A. Zdziarski<sup>\*</sup>

*N. Copernicus Astronomical Center, Bartycka 18, 00-716 Warszawa, Poland*

15 November 2018

## ABSTRACT

We investigate how the presence of a non-thermal tail beyond a Maxwellian electron distribution affects the synchrotron process as well as Comptonization in plasmas with parameters typical for accretion flows onto black holes. We find that the presence of the tail can significantly increase the net (after accounting for self-absorption) cyclo-synchrotron emission of the plasma, which emission then provides seed photons for Compton upscattering. Thus, the luminosity in the thermally-Comptonized spectrum is enhanced as well. The importance of these effects increases with both increasing Eddington ratio and the black hole mass. The enhancement of the Comptonized synchrotron luminosity can be as large as by factors of  $\sim 10^3$  and  $\sim 10^5$  for stellar and supermassive black holes, respectively, when the energy content in the non-thermal tail is 1 per cent.

The presence of the tail only weakly hardens the thermal Comptonization spectrum but it leads to formation of a high-energy tail beyond the thermal cut-off, which two effects are independent of the nature of the seed photons. Since observations of high-energy tails in Comptonization spectra can constrain the non-thermal tails in the electron distribution and thus the Comptonized synchrotron luminosity, they provide upper limits on the strength of magnetic fields in accretion flows. In particular, the measurement of an MeV tail in the hard state of Cyg X-1 by McConnell et al. implies the magnetic field strength in this source to be at most an order of magnitude below equipartition.

**Key words:** accretion, accretion discs – gamma-rays: theory – radiation mechanisms: thermal – X-rays: galaxies – X-rays: stars.

## 1 INTRODUCTION

Power-law-like X-ray spectra extending up to soft  $\gamma$ -rays (hereafter  $X\gamma$ ) are a common feature of the emission from accreting black holes in active galactic nuclei (AGNs) and black-hole binaries (BHBs). It is generally accepted that those spectra are produced by the Comptonization process taking place in optically thin accreting plasmas with typical electron energies of  $\sim 100$  keV. Similar spectra are also observed from weakly-magnetized accreting neutron stars (e.g. Barret et al. 2000), where they can originate either in the accretion flow or in a boundary layer near the neutron star surface.

The  $X\gamma$  spectra of Seyfert 1s and X-ray binaries in their hard (low) states can be modelled by Comptonization on thermal electrons, see e.g. Zdziarski (1999). However, both observations and theoretical considerations suggest that a

small non-thermal component may be present in the electron distribution, giving rise to a weak non-thermal high-energy tail in the observed Comptonization spectrum. Such a tail above  $\sim 1$  MeV has been detected in the spectrum of Cyg X-1 in the hard state by the COMPTEL detector aboard *CGRO* (McConnell et al. 1994, 2000a). In other BHBs and in Seyferts, the existing upper limits are compatible with the presence of weak non-thermal tails (e.g. Zdziarski et al. 1998; Gondek et al. 1996; Johnson et al. 1997).

A non-thermal tail in the electron distribution in compact  $X\gamma$  sources can arise due to many different physical mechanisms. One such mechanism is acceleration in the process of dissipation of magnetic field (similarly to the case of the solar corona) in an optically-thin accretion flow or in active coronal regions above an optically thick disc. Then, the energy loss and subsequent thermalization of the accelerated electrons leads to a steady-state electron distribution consisting of a Maxwellian and a non-thermal tail. Apart from Coulomb interactions, an effective thermalizing pro-

<sup>\*</sup> E-mail: gwar@camk.edu.pl (GW), aaz@camk.edu.pl (AAZ)

cess is synchrotron self-absorption (Ghisellini, Guilbert & Svensson 1988).

A strong support for the occurrence of non-thermal processes in black-hole accretion flows comes from observations of X $\gamma$  spectra of black-hole binaries in the soft state. In that case, Compton scattering by non-thermal electrons appears to be the dominant process (Poutanen & Coppi 1998; Gierliński et al. 1999). In the well-studied case of Cyg X-1, the power-law-like spectrum from this process becomes dominant at  $\gtrsim 10$  keV (Gierliński et al. 1999) and it extends to at least  $\sim 10$  MeV (McConnell et al. 2000b).

An important issue concerns the source of soft photons undergoing Comptonization in the accreting plasma. A natural candidate is thermal emission from an optically thick accretion disc, either below the corona or outside the region of optically thin accretion flow. However, as the presence of magnetic fields of the order of that corresponding to equipartition with gas pressure (i.e.  $\sim 10^3$  G in AGNs and  $\sim 10^7$  G in BHBs) is expected, one has to take into account Comptonization of synchrotron photons (hereafter the CS process) when calculating the emergent spectra. In models of advection-dominated accretion flows, the CS process may be the main radiative process in the innermost part of the accretion flow, where most of the available gravitational energy is liberated (e.g. Narayan & Yi 1995).

Wardziński & Zdziarski (2000, hereafter WZ00) have investigated the efficiency of the thermal CS process under physical conditions relevant for accreting black holes and found that it can dominate only in low-luminosity AGNs and in luminous stellar X-ray sources with the hardest spectra. In the latter case, however, the presence of a correlation between the spectral index and the strength of X-ray reflection (Zdziarski, Lubiński & Smith 1999; Gilfanov, Revnivtsev & Churazov 1999; Lubiński & Zdziarski 2001) appears to imply that blackbody emission of cold media is the main source of seed photons for thermal Comptonization, and the CS process is negligible.

In this work, we extend our previous results to the case of a hybrid, quasi-thermal plasma and investigate the influence of a weak non-thermal component in the electron distribution on the efficiency of the CS process. In Section 2, we discuss the shape of the electron distribution function resulting from acceleration processes operating in accretion flows. The influence of non-thermal tails on the CS emission of the plasma is discussed in Section 3. We then investigate in detail synchrotron emission and Comptonization spectrum of hybrid electrons in Sections 4 and 5.1, respectively. This allows us to estimate the efficiency of the CS process in hybrid plasmas (Section 5.2), and those results are applied to astrophysical black-hole sources in Section 5.3. Finally, we summarize our results in Section 6.

## 2 HYBRID ELECTRON DISTRIBUTIONS

In accretion flows, hybrid electron distributions can be produced e.g. by stochastic acceleration of thermal electrons by interaction with plasma instabilities, e.g. with whistlers via gyroresonance (as applied to the case of Cyg X-1 by Li, Kusunose & Liang 1996) or with fast-mode Alfvén waves via transit-time damping (Li & Miller 1997). Such process can result from dissipation of magnetic field in an accretion

disc corona (where magnetic fields are raised from the disc by buoyant forces, Galeev, Rosner & Vaiana 1979; Haardt, Maraschi & Ghisellini 1994) or in an optically thin accretion flow (Bisnovatyi-Kogan & Lovelace 1997), provided a significant fraction of the released energy generates turbulence.

Li & Miller (1997) considered parameters typical for a plasma in an accretion disc corona around a stellar black hole. They have shown, by solving the Fokker-Planck equation, that electrons can be effectively accelerated from the thermal background to relativistic energies, so that in the stationary state a non-thermal tail of a power-law-like shape develops above certain Lorentz gamma factor  $\gamma_{\text{nth}} \sim 2$  (which value is determined by the efficiency of thermalization processes, see Section 3,) and the power-law index,  $p$ , depends strongly on the plasma optical depth. The power-law component is cut off at a  $\gamma_f \sim 10$  due to radiative losses overcoming acceleration. Dermer, Miller & Li (1996) predict somewhat larger cut-off energies in the case of electron acceleration by whistlers and in a plasma with parameters relevant for AGNs.

Similar shape of steady-state electron distribution is also predicted from thermalization by synchrotron self-absorption and Coulomb interaction of an injected power-law electron distribution (produced by any acceleration mechanism), as shown by Ghisellini et al. (1988).

The exact shape of the non-thermal tail depends strongly on the plasma parameters and the (uncertain) mechanism of magnetic field dissipation and electron acceleration. We shall therefore consider a generic electron distribution function of the form qualitatively reproducing that predicted by detailed modelling of electron acceleration,

$$n_e(\gamma) = \begin{cases} n_e^{\text{th}}(\Theta, \gamma), & \gamma \leq \gamma_{\text{nth}}; \\ n_e^{\text{th}}(\Theta, \gamma_{\text{nth}}) \left(\frac{\gamma}{\gamma_{\text{nth}}}\right)^{-p} \exp\left(\frac{\gamma - \gamma_{\text{nth}}}{\gamma_f}\right), & \gamma > \gamma_{\text{nth}}. \end{cases} \quad (1)$$

Here  $\Theta \equiv kT/m_e c^2$  is the dimensionless electron temperature and  $n_e^{\text{th}}(\Theta, \gamma)$  is the relativistic Maxwellian normalized by the relation,  $n_e = \int_1^\infty n_e(\gamma) d\gamma$ , where  $n_e$  is the total electron density. This hybrid electron distribution consists thus of a thermal part below  $\gamma_{\text{nth}}$  and an e-folded power-law above it (see also Section 6).

We note that the cases  $p \lesssim 3$  and  $p > 3$  are qualitatively different. In the former, most of the non-thermal synchrotron luminosity is produced by electrons with  $\gamma \lesssim \gamma_f$  and the non-thermal synchrotron spectrum is hard. In the latter case, the luminosity is produced mostly by low-energy electrons,  $\gamma \sim \gamma_{\text{nth}}$ , and the spectrum is soft. Observations of Cyg X-1 (Gierliński et al. 1999; McConnell et al. 2000a) suggest  $p > 3$ . In the following we assume  $p \geq 3$ .

The degree to which a hybrid distribution is non-thermal can be measured by the quantity,  $(\gamma_{\text{nth}} - 1)/\Theta$ , which shows how far in the Maxwellian tail the non-thermal power law starts. Another such quantity is the ratio of the energy densities in the non-thermal and thermal parts of the electron distribution,  $\delta$ , which, for mildly relativistic temperatures and  $\gamma_{\text{nth}} - 1 \gg \Theta$  can be approximated as

$$\delta \approx \frac{\int_{\gamma_{\text{nth}}}^\infty (\gamma - 1)n_e(\gamma)d\gamma}{\frac{6+15\Theta}{4+5\Theta} \Theta n_e} \quad (2)$$

$$\approx \frac{4 + 5\Theta}{6 + 15\Theta} \frac{(\gamma_{\text{nth}}^2 - 1)^{1/2}}{\Theta^2 K_2\left(\frac{1}{\Theta}\right)} \left(\frac{\gamma_{\text{nth}}^3}{p-2} - \frac{\gamma_{\text{nth}}^2}{p-1}\right) e^{-\frac{\gamma_{\text{nth}}}{\Theta}},$$

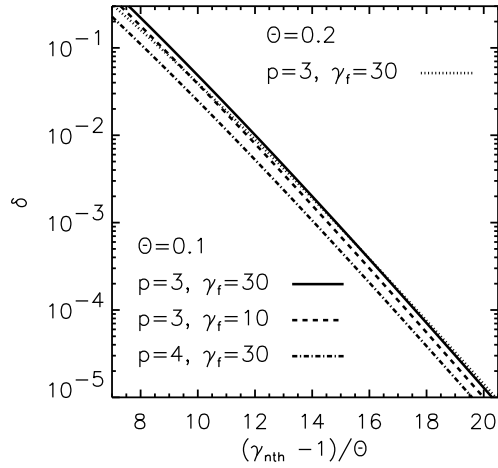


**Figure 1.** The relation between  $\gamma_{\text{nth}}$  and  $\delta$  for different plasma parameters.

where  $K_2$  is a modified Bessel function and we employed an approximation for the thermal energy density from Gammie & Popham (1998). In the above derivation (as well as in all analytical approximations below) we neglected, for simplicity, the exponential cut-off in the distribution (1). Typical relations between  $\delta$  and  $(\gamma_{\text{nth}} - 1)/\Theta$  are shown in Fig. 1.

Since the exponential term in equation (2) varies fastest, we have an approximate dependence,

$$\gamma_{\text{nth}} \approx C - \Theta \ln \delta, \quad (3)$$

where  $C \sim 1$  is slowly increasing with increasing  $\Theta$  and  $\gamma_{\text{nth}}$ . We then see that  $(\gamma_{\text{nth}} - 1)/\Theta$  only weakly depends on  $\Theta$  and the shape of the tail for a given  $\delta$ , see Fig. 1.

### 3 GENERAL FORM OF EMISSION FROM A HYBRID ELECTRON DISTRIBUTION

In accreting black holes, synchrotron emission from thermal plasmas optically thin to scattering is usually strongly self-absorbed up to a turnover frequency,  $\nu_t$ , below which the plasma is optically thick to absorption,

$$\alpha_{\nu_t} R = 1, \quad (4)$$

where  $\alpha_{\nu}$  is the absorption coefficient and  $R$  is the characteristic size of the source. Hereafter, we assume that  $\nu_t$  is determined only by synchrotron absorption, i.e. other radiative processes are negligible at  $\nu \sim \nu_t$ . Typically, accretion flow models predict (assuming equipartition magnetic fields)  $\nu_t \sim 10^{15}$  Hz for BHs and  $\nu_t \sim 10^{12}$  Hz for AGNs, see e.g. WZ00. This corresponds to the value of  $\nu_t/\nu_c$  from tens to hundreds, where  $\nu_c = eB/2\pi m_e c$  is the cyclotron frequency for the magnetic field of the strength  $B$  and  $m_e$  and  $c$  are, respectively, the rest mass of the electron and the velocity of light. The ratio,  $\nu_t/\nu_c$ , is larger in AGNs as a result of their magnetic field weaker than that in BHs. The Lorentz factor,  $\gamma_t$ , of the electrons that emit most of their synchrotron radiation at  $\nu_t$  is of the order of  $\gamma_t \sim (\nu_t/\nu_c)^{1/2}$ . The value

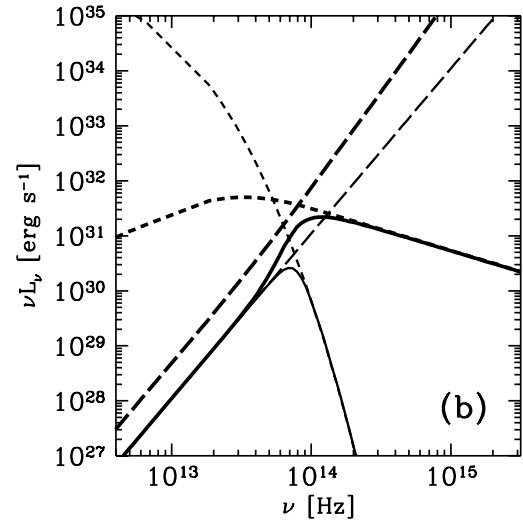
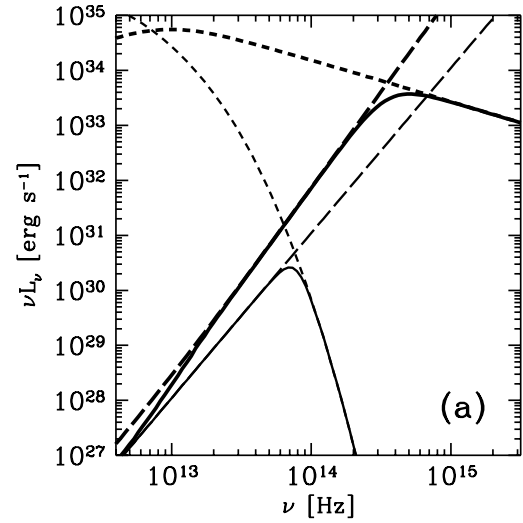


**Figure 2.** Synchrotron spectra from a spherical source with the energy content of the non-thermal tail of (a)  $\delta = 0.19$ , (b)  $\delta = 10^{-4}$ , and other plasma parameters as in our model of emission from Cyg X-1 in Section 5.3. The heavy short-dashed curve shows the optically-thin emission of the non-thermal electrons alone,  $(4/3)\pi R^3(4\pi j_{\nu}^{\text{pl}})$ , where  $j_{\nu}^{\text{pl}}$  is their emission coefficient. The heavy long-dashed curve shows the self-absorbed emission of the non-thermal electrons,  $4\pi^2 R^2 S_{\nu}^{\text{pl}}$ , where  $S_{\nu}^{\text{pl}}$  is their source function. The thin short-dashed and long-dashed curves show the thermal ( $\delta = 0$ ) optically-thin and optically-thick emission, respectively. The heavy and thin solid curves give the corresponding emergent spectra, which change from optically thick to optically thin around the turnover frequency.

of  $\gamma_t$  is of the order of a few, again larger in the case of AGNs than of BHs.

First, let us consider a homogenous cloud of thermal plasma. The CS spectrum below the thermal turnover frequency,  $\nu_t^{\text{th}}$ , can be approximated as a Rayleigh-Jeans spectrum. Above  $\nu_t^{\text{th}}$ , the synchrotron emission drops rapidly and the spectrum is often dominated by a power-law component resulting from Comptonization, which is cut off above an energy of  $\sim kT$ , where  $T$  is the electron temperature and  $k$  is the Boltzmann constant.

Now, let us assume that the electron distribution is given by equation (1). If  $\gamma_{\text{nth}} < \gamma_t$ , the number of electrons with  $\gamma \sim \gamma_t$  will increase (compared to the thermal case) as well as the absorption coefficient and in consequence the new turnover frequency,  $\nu_t^{\text{nth}}$ , will be larger. Also the shape of the synchrotron spectrum is modified in this case. At low frequencies both emission and absorption are dominated by thermal electrons so that the optically thick spectrum is still the Rayleigh-Jeans one. However, at higher frequencies the emission of non-thermal electrons starts to dominate, while absorption is still dominated by thermal electrons [which is a consequence of the thermal distribution falling off much more steeply than the non-thermal one, see equation (5)], and the optically-thick spectrum quickly increases. This leads to the regime in which both the non-thermal emission and absorption dominate, in which case the spectrum is proportional to the source function of non-thermal electrons. Finally, the spectrum becomes optically thin ( $\propto \nu^{-(p-1)/2}$ ), turning over above  $\nu_t^{\text{nth}}$ .

This behaviour is shown in Fig. 2 where the resulting synchrotron spectra are calculated for two different energy contents of the non-thermal tail and, as a reference, for the purely thermal case. Note that the non-thermal tail has to be sufficiently strong for the optically thick spectrum to reach the non-thermal source function before it turns over.

Both optically thick and optically thin parts of the synchrotron spectrum will undergo Comptonization. This process will thus be modified with respect to the thermal case due to two effects. Firstly, Compton scattering itself will involve both thermal electrons as well as non-thermal ones. The effect of non-thermal electrons on Comptonization will be most prominent at energies  $h\nu \gg kT$  (where  $h$  is the Planck constant), where a high-energy tail (above the thermal cut-off) will develop. Secondly, the seed-photon flux will be higher, so luminosity in the thermal Comptonization spectrum will also increase. Since  $\gamma_t$  in optically-thin plasmas around black holes is expected to be well above the mean energy of the thermal electrons, even a non-thermal tail carrying a tiny fraction of the total electron energy, and thus only weakly modifying the shape of the Comptonization spectrum, can increase the turnover frequency and thus the luminosity produced by the CS process by a large factor.

Then a question arises whether the presence of strong synchrotron self-absorption, acting as a thermalizing mechanism for electrons of  $\gamma \lesssim \gamma_t$  (i.e. in the regime of optically thick emission), will allow for an electron distribution deviating substantially from a pure Maxwellian for  $\gamma \sim \gamma_t$ . This issue was addressed by Ghisellini et al. (1988), who have shown that an initial power-law distribution of injected electrons will develop (after the thermalization time scale equal to a few synchrotron cooling timescales,  $t_c^{\text{syn}}$ , defined for the mean energy of the electrons radiating in the optically thick range of the spectrum) into a Maxwellian stationary distribution for  $\gamma < \gamma_t$ , provided the synchrotron cooling dominates and  $t_c^{\text{syn}} \ll t_{\text{esc}}$  (where  $t_{\text{esc}}$  is the escape time from the source). Assuming equipartition of magnetic field pressure with gas pressure, we find the latter criterion is always fulfilled in accretion flows onto black holes, independent of the form of the injected distribution.

However, when the inverse Compton process is dominant as a cooling mechanism, both  $\gamma_{\text{nth}}$  and  $kT$  diminish and a power-law tail starting below  $\gamma_t$  is formed, see

Ghisellini & Svensson (1990). A sufficient condition for the dominance of Compton cooling is  $\alpha < 1$ , which is typically fulfilled in astrophysical accreting black holes. Even when  $\alpha > 1$ , Comptonization of external soft photons (e.g. from a cold accretion disk) can dominate electron cooling (see, e.g. Ghisellini et al. 1998). Thus,  $\gamma_{\text{nth}} < \gamma_t$  is a likely condition in those sources.

#### 4 SYNCHROTRON TURNOVER FREQUENCY

Let  $\bar{\eta}_\nu(\gamma)$  be the synchrotron emission coefficient of a single electron averaged both over the electron velocity direction and the direction of emission. Then, the absorption coefficient for an isotropic distribution of electrons in a chaotic magnetic field is (e.g. Ghisellini & Svensson 1991) is

$$\alpha_\nu = \frac{-1}{2m_e\nu^2} \int_1^\infty \gamma (\gamma^2 - 1)^{\frac{1}{2}} \bar{\eta}_\nu(\gamma) \frac{d}{d\gamma} \left[ \frac{n_e(\gamma)}{\gamma(\gamma^2 - 1)^{\frac{1}{2}}} \right] d\gamma. \quad (5)$$

We assume a homogenous spherical source of the radius,  $R$ , and the Thomson optical depth,  $\tau_T$ , where  $\tau_T \equiv n_e\sigma_T R$  and  $\sigma_T$  is the Thomson cross section. Then, we can numerically calculate the absorption coefficient with equation (5) for the distribution of equation (1) and then solve equation (4) for the turnover frequency,  $\nu_t^{\text{nth}}$ . This can be compared with the *thermal* turnover frequency, which for plasma parameters typical for accreting black holes can be approximated as (WZ00)

$$\nu_t^{\text{th}} \approx 7 \times 10^3 \Theta^{0.95} \tau_T^{0.05} \nu_c^{0.91} \text{ Hz}. \quad (6)$$

On the other hand, we can obtain an analytical estimate,  $\nu_t^{\text{pl}}$ , of the turnover frequency for the hybrid electron distribution by considering a purely power-law electron distribution normalized to match the Maxwellian at  $\gamma_{\text{nth}}$ . For the synchrotron absorption coefficient for power-law electrons (Rybicki & Lightman 1979),

$$\nu_t^{\text{pl}} = 3^{\frac{1+p}{4+p}} 2^{-\frac{6}{4+p}} \pi^{\frac{1}{4+p}} \nu_c^{\frac{2+p}{4+p}} [G_1 R r_e c n_e (\gamma_{\text{nth}})^{\gamma_{\text{nth}}^p}]^{\frac{2}{4+p}}, \quad (7)$$

which, with equation (2), leads to

$$\nu_t^{\text{pl}} \approx 3^{\frac{1+p}{4+p}} 2^{-\frac{6}{4+p}} \pi^{\frac{1}{4+p}} \nu_c^{\frac{2+p}{4+p}} \left( \frac{\gamma_{\text{nth}}}{p-2} - \frac{1}{p-1} \right)^{-\frac{2}{4+p}} \times \left( \frac{6 + 15\Theta}{4 + 5\Theta} \frac{G_1 r_e c \tau_T \delta \Theta \gamma_{\text{nth}}^{p-1}}{\sigma_T} \right)^{\frac{2}{4+p}}, \quad (8)$$

where

$$G_1 = \frac{\Gamma(\frac{6+p}{4}) \Gamma(\frac{2+3p}{12}) \Gamma(\frac{22+3p}{12})}{\Gamma(\frac{8+p}{4})} \simeq 1, \quad (9)$$

$r_e$  is the classical electron radius and  $\Gamma$  is Euler's gamma function.

Provided  $p \gtrsim 3$  (so that radiation from electrons with  $\gamma > \gamma_f$  is negligible) and emission at  $\nu_t^{\text{nth}}$  is dominated by non-thermal electrons (i.e.  $\gamma_f > \gamma_t > \gamma_{\text{nth}}$ , which condition can be checked a posteriori by comparing the source function of power-law electrons to the Rayleigh-Jeans intensity),  $\nu_t^{\text{nth}} \simeq \nu_t^{\text{pl}}$ . On the other hand,  $\nu_t^{\text{pl}} < \nu_t^{\text{th}}$  when emission from thermal electrons is significant at  $\nu_t^{\text{nth}}$  and, in general,  $\nu_t^{\text{nth}} \simeq \max(\nu_t^{\text{th}}, \nu_t^{\text{pl}})$ .

The accuracy of this approximation is typically  $\lesssim 10$  per cent (provided  $\gamma_t < \gamma_f$  and  $p \gtrsim 3$ ). See WZ00 for a discussion of approximations of  $\nu_t^{\text{th}}$ .

We can obtain the dependences of  $\nu_t^{\text{nth}}/\nu_t^{\text{th}}$  on the plasma parameters by considering the ratio  $\nu_t^{\text{pl}}/\nu_t^{\text{th}}$  [given by approximations (6) and (7)]. First, at constant  $\delta$ , this ratio decreases with increasing  $\Theta$  since then  $\gamma_{\text{nth}}$  increases with  $\Theta$  [see equation (3)]. The dependence on  $\tau_T$  is stronger for  $\nu_t^{\text{pl}}$  than for  $\nu_t^{\text{th}}$  as a result of much steeper optically thin synchrotron spectrum in the latter case. This leads to  $\nu_t^{\text{pl}}/\nu_t^{\text{th}} \propto \tau_T^{2/(4+p)-0.05}$ , i.e. the larger the optical depth, the larger the ratio  $\nu_t^{\text{pl}}/\nu_t^{\text{th}}$ . In a hot accretion flow, we generally expect  $\tau_T$  increasing and  $\Theta$  decreasing with increasing accretion rate, so the effect of a non-thermal tail (of a given form) on the value of the turnover frequency can be expected to be the largest for the most luminous sources.

Since  $\nu_t^{\text{pl}}/\nu_t^{\text{th}} \propto \nu_c^{(2+p)/(4+p)-0.91}$ , the non-thermal increase of the turnover frequency grows with decreasing  $\nu_c$ . This effect is due to the increase of  $\gamma_t$  with decreasing  $\nu_c$  [as a result of increasing  $\nu_t^{\text{th}}/\nu_c$ , see equation (6)], which leads to a much larger ratio of the number of non-thermal to thermal electrons at  $\gamma_t$  for a given  $\gamma_{\text{nth}}$ . Thus, the effect of a non-thermal tail with a given form will be much stronger in AGNs than in BHBs (due to much weaker magnetic field in the former objects).

Fig. 3 shows the values of  $\nu_t^{\text{nth}}/\nu_t^{\text{th}}$  as a function of  $(\gamma_{\text{nth}} - 1)/\Theta$  for three sets of thermal plasma parameters. In the first and second set, we assume parameters relevant for luminous BHBs,  $\tau_T=1$ ,  $R = 3 \times 10^7$  cm,  $B = 10^7$  G, and  $\Theta = 0.1$  and  $0.2$ , respectively. In the third set, we assume parameters relevant to AGNs,  $\tau_T=1$ ,  $R = 3 \times 10^{14}$  cm,  $B = 10^3$  G and  $\Theta = 0.1$ . For each set, we consider two different slopes of the non-thermal tail,  $p = 3$  and  $4$  and  $\gamma_f = 30$ . Additionally, we consider the cases of  $\gamma_f = 10$  and  $100$  for  $p = 3$  (for  $p > 3$  the influence of the cut-off is much weaker). We see that even a weak non-thermal component, with  $(\gamma_{\text{nth}} - 1)/\Theta \sim 12$  (which corresponds to only  $\sim 1$  per cent of the total energy density of the electrons in the non-thermal tail) can lead to an increase of the turnover frequency by a factor of  $\sim 1.5$ - $2$  for BHBs and  $\sim 10$  for AGNs.

The dependence of the relative increase of the turnover frequency on  $p$  and  $\gamma_f$  is relatively weak. This reflects the fact that the turnover frequency depends mostly on the number of electrons at  $\gamma_t$  and since for small values of  $\delta$ ,  $\gamma_t$  is only slightly larger than  $\gamma_{\text{nth}}$ ,  $n_e(\gamma_t)$  depends weakly on either  $p$  or  $\gamma_f$ . This suggests that the degree of the dependence on  $p$  and  $\gamma_f$  should increase with increasing  $\nu_t^{\text{nth}}/\nu_t^{\text{th}}$ , in agreement with our results. It is important to note that weak dependence of  $\nu_t^{\text{nth}}/\nu_t^{\text{th}}$  on the shape of the non-thermal tail makes our results weakly dependent on details of the acceleration mechanism.

## 5 COMPTONIZATION BY A HYBRID ELECTRON DISTRIBUTION

### 5.1 The general case

For Comptonization by a thermal plasma, we employ here a simple treatment of this process of Zdziarski (1985, 1986). In that approximation, the Comptonization spectrum above

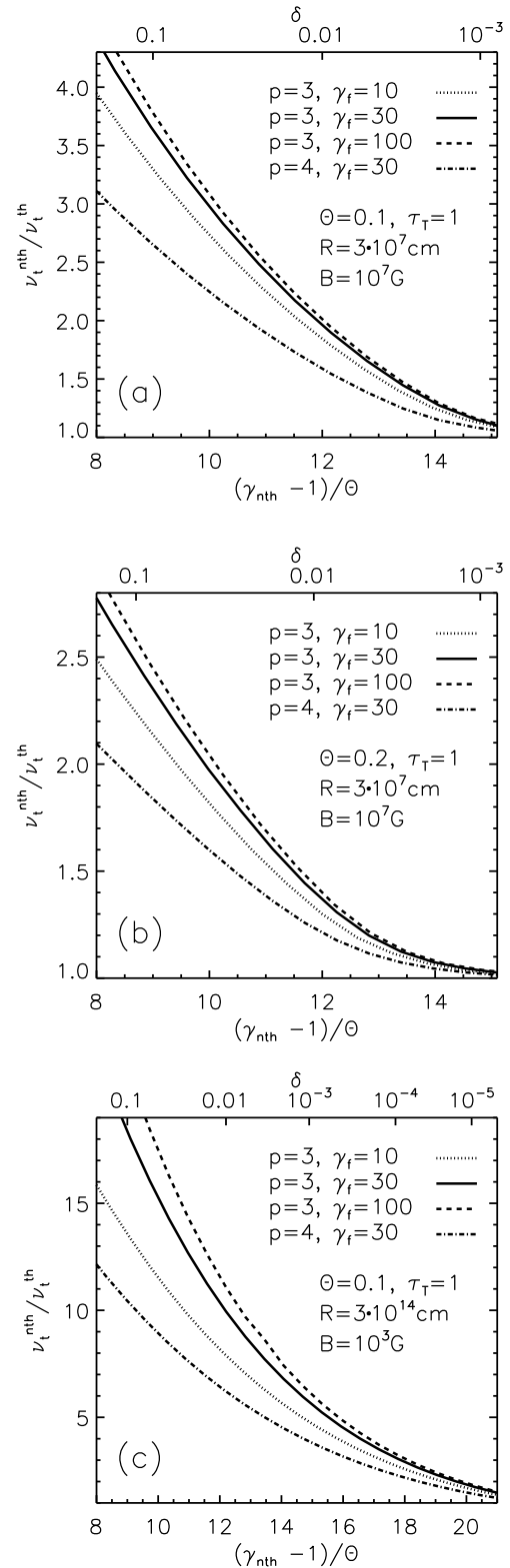


**Figure 3.** The increase of  $\nu_t$  as a function of the electron energy where the non-thermal tail starts for various plasma parameters and forms of the tail. The upper axis shows the values of  $\delta$  for  $p = 3$  and  $\gamma_f = 30$ . Note that the relation between  $(\gamma_{\text{nth}} - 1)/\Theta$  and  $\delta$  is slightly different for the curves with other values of  $p$  and  $\gamma_f$ , see Fig. 1.

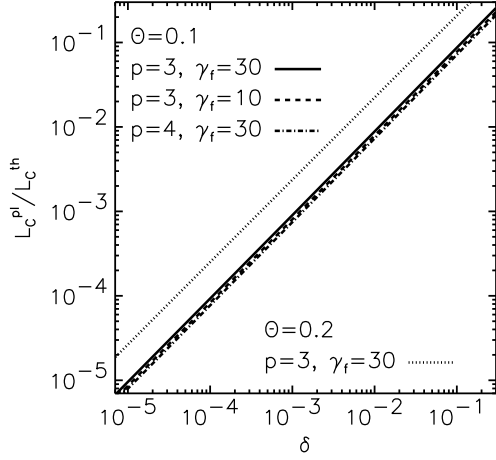


**Figure 4.** The relation between the fraction of energy carried by non-thermal electrons and the ratio of  $L_C^{\text{pl}}/L_C^{\text{th}}$  for different plasma parameters and  $\alpha = 0.7$ .

the frequency,  $\nu_{\text{inj}}$ , at which soft seed photons are injected (which, in the case of the CS process,  $\approx \nu_t^{\text{th}}$ ), can be approximated as a sum of an  $e$ -folded power-law with energy index  $\alpha$  and a Wien spectrum,

$$\frac{dL_C^{\text{th}}}{dx} \propto \left[ \left( \frac{x}{\Theta} \right)^{-\alpha} + \frac{\Gamma(\alpha)P_{\text{sc}}}{\Gamma(2\alpha+3)} \left( \frac{x}{\Theta} \right)^3 \right] e^{-x/\Theta}, \quad (11)$$

where  $x \equiv h\nu/m_e c^2$  (hereafter all indices of  $x$  have the same meaning as those of  $\nu$ ) and  $P_{\text{sc}}$  is the volume-averaged scattering probability. Its integration yields the thermal-Compton luminosity, which, in the case of a spherical source, is

$$L_C^{\text{th}}(C) \simeq 4\pi R^2 \mathcal{C} \Theta \left[ \Gamma \left( 1 - \alpha, \frac{x_{\text{inj}}}{\Theta} \right) + \frac{6\Gamma(\alpha)P_{\text{sc}}}{\Gamma(2\alpha+3)} \right], \quad (12)$$

where  $\mathcal{C}$  is a constant depending on the flux of the injected seed photons (we calculate  $\mathcal{C}$  in Section 5.2 for the case of synchrotron seed photons).

The presence of non-thermal electrons modifies the Comptonization spectrum and since for the electron distributions we consider (i.e.  $\tau_T \sim 1$  and  $\delta \ll 1$ ) the Thomson optical depth for scattering off non-thermal electrons is  $\ll 1$ , the resulting spectrum can be approximated as a convolution of the thermal Comptonization spectrum with a spectrum resulting from single scattering of photons off non-thermal electrons. Therefore, for  $x \lesssim \Theta$ , the Comptonization spectrum becomes harder, while for  $x \gg \Theta$ , above the thermal cut-off, a power-law tail in the spectrum develops. As a result, the overall luminosity produced by Comptonization increases.

In calculations of the luminosity from Comptonization on non-thermal electrons,  $L_C^{\text{pl}}$ , where the Klein-Nishina effect has to be taken into account, we use the approximation for the rate of energy change,  $d\gamma/dt$ , of a single electron via Compton interaction with isotropic photons of energy density,  $U_{\text{ph}}$ , and mean energy,  $\langle x \rangle$ ,

$$\frac{d\gamma}{dt} = -\frac{4}{3} \frac{\sigma_T (\gamma^2 - 1) U_{\text{ph}}}{m_e c} \left[ 1 - \frac{63}{10} \frac{\gamma \langle x^2 \rangle}{\langle x \rangle} \right], \quad (13)$$

where the Klein-Nishina cross-section was approximated using the first-order correction to the Thomson-limit cross-section (Rybicki & Lightman 1979). We assume that the photons undergoing scattering off non-thermal electrons are those from the thermal Comptonization spectrum above  $x_{\text{inj}}$ . Then

$$U_{\text{ph}}(x) = \frac{3 (dL_C^{\text{th}}/dx) (3/4 + \tau_T/5)}{4\pi c R^2}, \quad (14)$$

where the factor  $(3/4 + \tau_T/5)$  accounts for the change of the escape time due to scatterings in the source and is a matching formula between the optically thin case (where the escape time is  $3R/4c$ ) and the optically thick one ( $\tau_T R/5c$ , Sunyaev & Titarchuk 1980). We can further simplify the calculations assuming that the spectrum of photons undergoing non-thermal Comptonization is a pure power-law and then neglect scatterings in the Klein-Nishina limit (see below).

Now, for each  $\gamma$  we calculate  $U_{\text{ph}}$ ,  $\langle x \rangle$  and  $\langle x^2 \rangle$  as an integral over the power-law spectrum from  $x_{\text{inj}}$  up to the energy,  $x_{\text{max}}$ , of the limit of the Klein-Nishina regime, which we obtain from the condition of  $1 - 63/(10\gamma x_{\text{max}}) = 0$ , in which the numerical coefficient is chosen for consistency with equation (13).

Then the formula (13) is integrated over  $n_e(\gamma)$ , from  $\gamma_{\text{nth}}$  to infinity, which leads to

$$L_C^{\text{pl}}(C) = \frac{16\pi}{3} \left( \frac{10}{63} \right)^{1-\alpha} \frac{6 + 15\Theta}{4 + 5\Theta} \left( \frac{3}{4} + \frac{\tau_T}{5} \right) \frac{R^2 \mathcal{C} \delta \tau_T \Theta^{\alpha+1}}{(1-\alpha)(2-\alpha)} \times \left( \frac{\gamma_{\text{nth}}}{p-2} - \frac{1}{p-1} \right)^{-1} \left( \frac{\gamma_{\text{nth}}^{\alpha+1}}{p-\alpha-2} - \frac{\gamma_{\text{nth}}^{\alpha-1}}{p-\alpha} \right), \quad (15)$$

where equation (2) has been employed.

The total luminosity,  $L_C^{\text{th}} = L_C^{\text{th}} + L_C^{\text{pl}}$ , as well as the ratio  $L_C^{\text{pl}}/L_C^{\text{th}}$  can now be directly obtained from expressions (12) and (15). In the range of  $0.4 \lesssim \alpha \lesssim 0.9$ , both the high-energy part of the power law component dominates the luminosity as well as the Wien component can still be neglected. Then, we obtain (see WZ00)

$$\frac{L_C^{\text{pl}}}{L_C^{\text{th}}} \approx \frac{4}{3} \left( \frac{10}{63} \right)^{1-\alpha} \frac{6 + 15\Theta}{4 + 5\Theta} \left( \frac{3}{4} + \frac{\tau_T}{5} \right) \frac{\delta \tau_T \Theta^\alpha}{2-\alpha} \times \left( \frac{\gamma_{\text{nth}}}{p-2} - \frac{1}{p-1} \right)^{-1} \left( \frac{\gamma_{\text{nth}}^{\alpha+1}}{p-\alpha-2} - \frac{\gamma_{\text{nth}}^{\alpha-1}}{p-\alpha} \right). \quad (16)$$

We find the accuracy of this approximation is typically  $\lesssim 30$  per cent. Figure 4 shows that while the ratio  $L_C^{\text{pl}}/L_C^{\text{th}}$  depends strongly on  $\delta$ , the dependence on the non-thermal tail shape is very weak.

In Fig. 5, we show as an example Comptonization spectra from a homogenous plasma cloud, produced with the Monte Carlo code of Gierliński (2000). We see that as long as  $\delta < 0.1$  the Comptonization spectrum at  $x \lesssim \Theta$  is hardly modified by the presence of non-thermal electrons and the onset of the power-law tail is no higher than an order of magnitude below the peak in the  $xL(x)$  spectrum.

From the observational point of view, an important feature measuring the deviation from purely thermal Comptonization spectrum is the fraction of the luminosity radiated in the high-energy tail beyond the thermal spectrum.

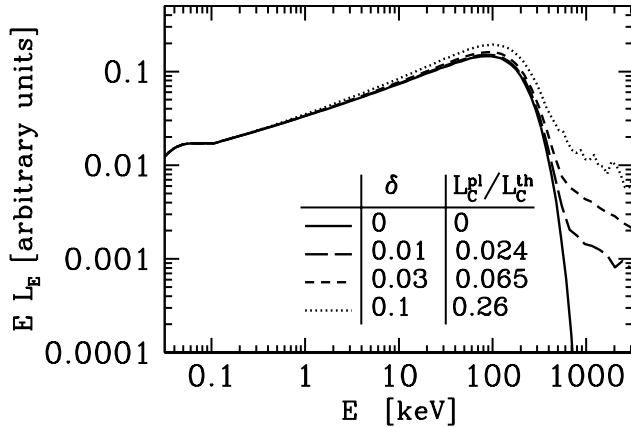


**Figure 5.** Monte Carlo Comptonization spectra of 10-eV black-body photons in a plasma of  $\Theta = 0.1$ ,  $\tau_T = 2.4$ . The solid line represents the thermal spectrum, while the other lines correspond to the cases of power-law tails in the electron distribution of  $p = 3$ ,  $\gamma_f = 30$  and different values of  $\delta$ .

The ratio  $L_C^{\text{pl}}/L_C^{\text{th}}$  is larger than this fraction as it incorporates also the non-thermal luminosity at energies below the tail. This effect is stronger for smaller  $\delta$ , when a larger fraction of  $L_C^{\text{pl}}$  is hidden below the thermal peak. For example, in the spectra in Fig. 5 corresponding to  $\delta = 0.1$  and  $\delta = 0.01$  the high-energy tail develops at  $\sim 300$  keV and  $\sim 500$  keV, respectively. Then  $L_C^{\text{pl}}/L_C^{\text{th}}$  is larger than the fraction of the luminosity in the tail by factors 3 and 5, respectively. Thus,  $L_C^{\text{pl}}/L_C^{\text{th}}$  provides only an upper limit to the fraction of the luminosity radiated in the high-energy tail.

## 5.2 Comptonization of synchrotron photons

As we have seen above, the presence of a non-thermal component in the thermal distribution of electrons in a plasma where synchrotron radiation is produced and then Comptonized leads to an increase of the luminosity available from this process in two ways. First, it increases the number of soft photons (both from optically thick emission up to  $x_t^{\text{nth}}$  and from optically thin emission above  $x_t^{\text{nth}}$ ) and second, it increases the efficiency of Comptonization, the former effect being significantly stronger.

In the case of purely thermal synchrotron Comptonization, the normalization of the Comptonization spectrum can be assumed (Zdziarski 1985, 1986) to be proportional to the Rayleigh-Jeans flux at the turnover frequency, so that the constant  $\mathcal{C}$  in the expression (12), which we now denote as  $\mathcal{C}^{\text{th}}$ , reads,

$$\mathcal{C}^{\text{th}} = \frac{2\pi m_e c^3}{\lambda_C^3} \varphi \Theta^{1-\alpha} (x_t^{\text{th}})^{2+\alpha}, \quad (17)$$

where

$$\varphi(\Theta) \approx \frac{1 + (2\Theta)^2}{1 + 10(2\Theta)^2} \quad (18)$$

is a heuristic formula obtained by Zdziarski (1985) to match Monte Carlo simulation, and  $\lambda_C$  is the Compton wavelength. The total luminosity from the CS process is then

$$L_{\text{CS}}^{\text{th}} = L_S^{\text{th}} + L_C^{\text{th}}(\mathcal{C}^{\text{th}}), \quad (19)$$

where  $L_S^{\text{th}}$  is the luminosity in the thermal synchrotron spectrum.

If thermal and hybrid synchrotron photons experience the same average number of scatterings off thermal electrons before reaching  $x \sim \Theta$  (i.e. when  $x_t^{\text{nth}}/x_t^{\text{th}} \ll \Theta/x_t^{\text{th}}$  and the synchrotron spectrum is sufficiently narrow, which corresponds to  $p > 3$  and which we assume hereafter in this section), the ratio of the luminosity from Comptonization off thermal electrons in the hybrid case to that in the thermal case will equal the corresponding ratio of the synchrotron luminosities. Then,

$$\frac{\mathcal{C}^{\text{nth}}}{\mathcal{C}^{\text{th}}} = \frac{L_S^{\text{nth}}}{L_S^{\text{th}}}, \quad (20)$$

where  $L_S^{\text{nth}}$  is the hybrid synchrotron luminosity and  $\mathcal{C}^{\text{nth}}$  is the normalization constant for thermal Comptonization spectrum of hybrid synchrotron photons.

To calculate the ratio (20) we assume the optically thick hybrid synchrotron emission below  $x_t^{\text{nth}}$  to be  $\propto S^{\text{pl}}(x)$ , the source function of power-law electrons,

$$S^{\text{pl}}(x) = \frac{1}{2} \frac{G_2}{3^{1/2}} \frac{m_e c^3}{G_1 \lambda_C^3} x_c^{-1/2} x^{5/2}, \quad (21)$$

where

$$G_2 = \frac{\Gamma(\frac{5+p}{4})\Gamma(\frac{3p+19}{12})\Gamma(\frac{3p-1}{12})}{\Gamma(\frac{7+p}{4})} \simeq 1. \quad (22)$$

The emission above  $\nu_t^{\text{nth}}$  is  $\propto \nu^{-(p-1)/2}$  and then we have

$$\frac{\mathcal{C}^{\text{nth}}}{\mathcal{C}^{\text{th}}} = \frac{3^{1/2}(p+4)G_2 (x_t^{\text{nth}}/x_c)^{7/2}}{14(p-3)G_1\Theta (x_t^{\text{th}}/x_c)^3}. \quad (23)$$

The above expressions were derived using the emission and absorption coefficients for power-law electrons (e.g. Rybicki & Lightman 1979). Since we neglected the cut-off in the electron distribution, the above relation holds for  $x_t^{\text{nth}}/x_c \ll \gamma_f^2$ , i.e. when the contribution from electrons with  $\gamma > \gamma_f$  to the emission at  $x_t^{\text{nth}}$  can be neglected.

The total luminosity of the CS process in the hybrid case is then

$$L_{\text{CS}}^{\text{nth}} = L_S^{\text{nth}} + L_C^{\text{th}}(\mathcal{C}^{\text{nth}}) + L_C^{\text{pl}}(\mathcal{C}^{\text{nth}}). \quad (24)$$

When  $\alpha < 1$ , we can neglect  $L_S^{\text{th}}$  and  $L_S^{\text{nth}}$  in equations (19) and (24) respectively, since most of the luminosity is then produced at much higher energies,  $x \sim \Theta$ . Then, the ratio  $L_{\text{CS}}^{\text{nth}}/L_{\text{CS}}^{\text{th}}$  can be calculated as

$$\frac{L_{\text{CS}}^{\text{nth}}}{L_{\text{CS}}^{\text{th}}} = \frac{\mathcal{C}^{\text{nth}}}{\mathcal{C}^{\text{th}}} \left[ 1 + \frac{L_C^{\text{pl}}(\mathcal{C}^{\text{th}})}{L_C^{\text{th}}(\mathcal{C}^{\text{th}})} \right]. \quad (25)$$

We can neglect the last term in the brackets if  $\delta$  is sufficiently small, in which case  $L_C^{\text{pl}}(\mathcal{C}^{\text{th}}) \ll L_C^{\text{th}}(\mathcal{C}^{\text{th}})$ . We then have

$$\frac{L_{\text{CS}}^{\text{nth}}}{L_{\text{CS}}^{\text{th}}} \approx \frac{3^{1/2}(p+4) (x_t^{\text{nth}}/x_c)^{7/2}}{14(p-3)\Theta (x_t^{\text{th}}/x_c)^3}. \quad (26)$$

Note that in calculations of  $\mathcal{C}^{\text{nth}}$  we used the source function for power-law electrons. Thus, this approximation does not have the correct thermal limit when  $\gamma_{\text{nth}} \gg \gamma_t$ , i.e. when  $x_t^{\text{nth}} \approx x_t^{\text{th}}$  (see Fig. 2b, where a synchrotron spectrum for such a case is shown). Note also that for harder power-law electron distributions ( $p \lesssim 3$ ), for which the approximation

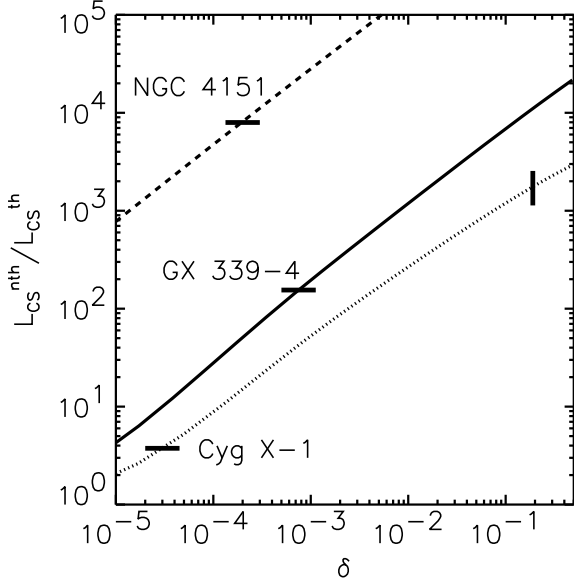


**Figure 6.** The amplification of the CS emission due to the presence of nonthermal electrons,  $L_{\text{CS}}^{\text{nth}}/L_{\text{CS}}^{\text{th}}(\delta)$ , for models (see text) of NGC 4151, GX 339-4 and Cyg X-1 (dashed, solid and dotted curves, respectively). The horizontal lines correspond to the amplification required to account for the observed X-ray luminosities and the corresponding values of  $\gamma_{\text{nth}}$  are 2.61, 2.46, and 4.10 in the above 3 objects, respectively. The vertical line corresponds to  $\delta$  obtained from observations of the non-thermal tail in the spectrum of Cyg X-1 by McConnell et al. (2000a), which corresponds to the X-ray luminosity exceeding that observed by a factor of  $\sim 500$ .

(20) does not hold, the amplification of CS luminosity will be even larger than that predicted above.

### 5.3 Applications to NGC 4151, GX 339-4 and Cyg X-1

We now calculate the ratio  $L_{\text{CS}}^{\text{nth}}/L_{\text{CS}}^{\text{th}}$  as a function of the energy content of the electron power-law tail in three different cases. They correspond to the models of thermal CS emission from a hot accretion disc with magnetic field in equipartition with the gas internal energy (dominated by hot ions) of WZ00 for the Seyfert galaxy NGC 4151 and two BHs in their hard states, GX 339-4 and Cyg X-1. The CS luminosities predicted by the thermal model (fig. 8a in WZ00) were orders of magnitude below the ones observed from NGC 4151 and GX 339-4, and less by a factor of  $\sim 3$  for Cyg X-1.

For NGC 4151, we assume (see WZ00 for details and references)  $R = 1.2 \times 10^{14}$  cm,  $B = 3.8 \times 10^3$  G,  $\alpha = 0.85$ ,  $\Theta = 0.1$ ,  $p = 4$ ,  $\gamma_f = 100$ . For GX 339-4, the same values of  $\Theta$ ,  $p$  and  $\gamma_f$  are adopted while  $R = 8.8 \times 10^6$  cm,  $B = 1.5 \times 10^7$  G,  $\alpha = 0.75$ . In the case of Cyg X-1,  $R = 3 \times 10^7$  cm,  $B = 6.3 \times 10^6$  G,  $\alpha = 0.6$ , and we use the electron distribution obtained in McConnell et al. (2000a) by fitting the spectra from the COMPTEL and OSSE detectors aboard *CGRO*, i.e.  $\Theta = 0.17$ ,  $\gamma_{\text{nth}} = 2.12$ ,  $p = 4.5$ , at assumed  $\gamma_f = 10^3$ , which corresponds to a rather large value of  $\delta = 0.19$ .

The results are shown in Fig. 6. In the case of NGC 4151 and GX 339-4, a non-thermal tail in the electron distribution with  $\delta \lesssim 10^{-3}$  amplifies the power produced by the CS process sufficiently to reproduce the luminosities of those sources. Therefore, unlike the results obtained by WZ00 from investigating the purely thermal CS process, in the case of electron distributions with relatively weak non-thermal tails the CS process appears to be capable of producing the observed X-ray spectra of accreting black holes, independent of the Eddington ratio or the black hole mass.

On the other hand, the estimated *thermal* CS luminosity in the case of Cyg X-1 in the hot disc model is comparable to that observed from the source. Then, we find that the non-thermal tail observed by McConnell et al. (2000a) would produce the CS luminosity  $\sim 500$  times higher than that actually observed (see Fig. 2a, where thermal and hybrid synchrotron spectra are plotted for plasma parameters assumed in this model). The requirement that  $L_{\text{CS}}^{\text{nth}}$  cannot exceed the source luminosity constrains the magnetic field strength in the model to be  $B \lesssim 2.3 \times 10^5$  G, which is  $\sim 30$  times smaller than the equipartition value estimated by WZ00.

A similar constraint for Cyg X-1 can be obtained in a model of active coronal regions above the disc with magnetic field dissipation (see WZ00 for details of the corresponding model of CS emission). Assuming  $N = 10$  active regions of radius  $R_b = 3 \times 10^6$  cm and height  $H_b = 3 \times 10^5$  cm, we obtain  $B \lesssim 3.4 \times 10^6$  G, much less than the field strength predicted assuming dissipation of magnetic field at a fraction of the Alfvén speed,  $B_{\text{diss}} = 5 \times 10^7$  G. Though varying  $N$ ,  $R_b$ ,  $H_b$  would change the upper limit on the field strength as well as the value of  $B_{\text{diss}}$ , the relation between these quantities would remain similar. This suggests that the mechanism of dissipation of disc field in small active regions above the disc cannot be responsible for the energy release in the corona. This stems from the fact that  $B_{\text{diss}}$  is the minimum field strength necessary for the magnetic field to dissipate enough energy so as to produce the observed luminosity. Therefore, either the model of active regions above a cold disc is ruled out for the hard state of Cyg X-1 or another mechanism of energy release must operate. We point out that if the CS process were to be negligible (as suggested by observations, see Section 6), the magnetic field would have to be even weaker, which would strengthen our conclusion even more. On the other hand, a weak magnetic field does not present analogous difficulties in the hot accretion disc model as the disc heating is directly by gravity.

We then check how sensitive the above results are to details of the observed spectra of Cyg X-1. First, the spectral index of Cyg X-1 varies, and the value  $\alpha = 0.6$  assumed above is the hardest one and spectra with  $\alpha = 0.7$  have been also observed. Second, the relative normalization between the COMPTEL and OSSE spectra remains relatively uncertain, and it may be possible that the former is less by  $\sim 2$  (McConnell et al. 2000b) than the one used in the calculations above. This would then diminish the energy content in the electron non-thermal tail twice, which corresponds to the new value of  $\gamma_{\text{nth}} = 2.31$ . Thus, we have repeated our calculations for  $\alpha = 0.7$  and  $\gamma_{\text{nth}} = 2.31$ . The resulting constraints on the magnetic field strength in the hot disc and active regions models are then  $B \lesssim 5.8 \times 10^5$  G and  $B \lesssim 6.8 \times 10^6$  G, respectively. These values are only about



twice the previous upper limits, which does not affect our conclusions above.

We note that another constraint on the CS emission may be provided by extrapolating the X-ray power law spectrum to lower energies (but  $\gtrsim h\nu_i$ ), e.g. to the UV or optical ranges. That emission should not, in any case, exceed that observed. In the case of Cyg X-1, we have extrapolated the observed X-ray power-law spectrum of Cyg X-1 (Gierliński et al. 1997) to  $\nu \simeq 10^{15}$  Hz and have found it is more than 2 orders of magnitude below the UV spectrum of the companion supergiant as observed by *IUE* (Treves et al. 1980). Thus, those data are compatible with the CS origin of the X-ray spectrum in Cyg X-1.

On the other hand, GX 339-4 is a low-mass X-ray binary with a low upper limit on the emission of the companion star (e.g. Zdziarski et al. 1998). Then, simultaneous (as the object is highly variable, e.g. Corbet et al. 1987) observations in X-rays and at longer wavelengths can put constraints on the CS model in this case (e.g. Fabian et al. 1982).

## 6 CONCLUSIONS AND DISCUSSION

We have studied the influence of non-thermal tails in the electron distribution on the Comptonized synchrotron emission from plasmas of parameters typical for accreting black holes. In those plasmas, most of the self-absorbed thermal synchrotron emission is produced by electrons far in the tail of the Maxwellian distribution. As a result, even a weak non-thermal component far beyond the thermal peak can greatly enhance the synchrotron emission. This emission provides seed photons for Comptonization, which is also correspondingly enhanced. However, the shape the Comptonization spectrum remains only weakly modified, with the main signature being a relatively weak high-energy tail.

We have shown that this effect becomes stronger with the decreasing plasma temperature and increasing optical depth, which typically correspond to an increasing Eddington ratio. It is also much stronger in the case of AGNs than of accreting stellar black holes, as a result of weaker magnetic field in the former objects. The CS luminosity can be amplified by a factor  $\sim 10^5$  and  $\sim 10^3$ , respectively, in the case of only  $\sim 1$  per cent of the electron energy in the non-thermal tail.

Then, the Comptonized synchrotron emission becomes energetically capable of producing the observed luminosities of accreting black holes independently of their Eddington ratio or the black-hole mass. This conclusion is qualitatively different from that obtained in the case of purely thermal plasma.

It is then possible to obtain upper limits on the magnetic field strength in optically thin plasmas around black holes by constraining the parameters of the non-thermal component in the electron distribution from observations of the high-energy tail in Comptonization spectra. Based on the *CGRO* data for Cyg X-1 in the hard state, we have obtained the upper limits on the field strength at least an order of magnitude below both the value corresponding to equipartition (in the model of a two-temperature accretion disc) and the minimum value required by dissipation of magnetic fields (in the model of active coronal regions). There-

fore, the latter model appears to be ruled out for the hard state of Cyg X-1.

We note that the presence of a strong correlation between reflection strength and the X-ray spectral index, observed in Cyg X-1 (Gilfanov et al. 1999), suggests that the CS emission is a negligible source of photons for Comptonization and thus the magnetic field strength must remain significantly below the upper limits derived above. The same correlation seen in other objects (Zdziarski et al. 1999; Gilfanov et al. 2000) implies that either the high-energy tails or the magnetic fields are weak enough for the CS process not to dominate the energy output.

In this work, we have assumed, for the sake of simplicity and compatibility with studies of, e.g., McConnell et al. (2000a), the electron distribution of the non-thermal electron tails to be  $\propto \gamma^{-p}$  at any value of  $\gamma$ . However, when the power-law tail extends down to non-relativistic energies,  $\gamma_{\text{nth}} \sim 1$ , the distributions expected from acceleration processes are power laws in either the kinetic energy or the momentum, e.g.  $\propto (\gamma - 1)^{-p}$  for the former. Clearly, the smaller  $\gamma_{\text{nth}}$  (i.e. the larger  $\delta$ ), the larger the differences between those distributions. Then, the actual shift of the turnover frequency at a given value of  $\gamma_{\text{nth}}$  would be somewhat smaller. Also, the relation between  $\gamma_{\text{nth}}$  and  $\delta$  would change. Nevertheless, the above effects would modify our results only quantitatively without affecting our conclusions.

The influence of a weak, non-thermal, component in the electron distribution on radiation spectra has also been independently considered by Özel, Psaltis & Narayan (2000). Their study has been devoted to the case of advection-dominated accretion flows (ADAF), and their presented spectra are integrated over all radii of the flow. In contrast to our results, they do not note any shift in the turnover frequency at the peak of the synchrotron spectrum. This appears to result from their study being constrained to the ADAF model at low accretion rates, in which case electrons in the innermost parts of the accretion flow reach rather high temperatures (at which even thermal electrons reach relatively high Lorentz factors). Those temperatures are significantly higher than those we consider based on observational data from luminous accreting black holes. On the other hand, Özel et al. (2000) find a significant excess non-thermal emission at frequencies well below the peak of the integrated synchrotron spectrum. This excess results from radiation emitted at large radii, where the electron temperature is low, and where the synchrotron emission (both optically thick and optically thin) around the local turnover frequency can be strongly amplified by the presence of an electron tail, as illustrated in Fig. 2 above.

## ACKNOWLEDGMENTS

This research has been supported in part by the Foundation for Polish Science and KBN grants 2P03D01619 and 2P03D00624. We thank Marek Gierliński for providing us with his Monte-Carlo Comptonization code and for help with its use. We are also grateful to Andrei Beloborodov, Joanna Mikołajewska and Juri Poutanen for valuable discussions.

## REFERENCES

- Barret D., Olive J. F., Boirin L., Done C., Skinner G. K., Grindlay J. E., 2000, *ApJ*, 533, 329
- Bisnovatyi-Kogan G. S., Lovelace R. V. E., 1997, *ApJ*, 486, L43
- Corbet R. H. D., Thorstensen J. R., Charles P. A., Honey W. B., Smale A. P., Menzies J. W., 1987, *MNRAS*, 227, 1055
- Dermer C. D., Miller J. A., Li H., 1996, *ApJ*, 456, 106
- Fabian A. C., Guilbert P. W., Motch C., Ricketts M., Ilovaisky S. A., Chevalier C., 1982, *A&A*, 111, L9
- Galeev A. A., Rosner R., Vaiana G. S., 1979, *ApJ*, 229, 318
- Gammie C. F., Popham R., 1998, *ApJ*, 498, 313
- Ghisellini G., Svensson R., 1990, in Brinkmann W. et al., eds., *Physical Processes in Hot Cosmic Plasmas*. Kluwer Academic Publishers, p. 395
- Ghisellini G., Svensson R., 1991, *MNRAS*, 252, 313
- Ghisellini G., Guilbert P. W., Svensson R., 1988, *ApJ*, 334, L5
- Ghisellini G., Haardt F., Svensson R., 1998, *MNRAS*, 297, 348
- Gierliński M., 2000, PhD thesis, N. Copernicus Astron. Center, Warsaw
- Gierliński M., Zdziarski A. A., Done C., Johnson W. N., Ebisawa K., Ueda Y., Haardt F., Philips B. F., 1997, *MNRAS*, 288, 958
- Gierliński M., Zdziarski A. A., Poutanen J., Coppi P. S., Ebisawa K., Johnson N. W., 1999, *MNRAS*, 309, 496
- Gilfanov M., Churazov E., Revnivtsev M., 1999, *A&A*, 352, 182
- Gilfanov M., Churazov E., Revnivtsev M., 2000, in *Proc. 5th CAS/MPG Workshop on High Energy Astrophysics*, in press (astro-ph/0002415)
- Gondek D., Zdziarski A. A., Johnson W. J., George I. M., McNaron-Brown K., Magdziarz P., Smith D., Gruber D. E., 1996, *MNRAS*, 282, 646
- Grove J. E. et al., 1998, *ApJ*, 500, 899
- Haardt F., Maraschi L., Ghisellini G., 1994, *ApJ*, 432, L95
- Johnson W. N., McNaron-Brown K., Kurfess J. D., Zdziarski A. A., Magdziarz P., Gehrels N., 1997, *ApJ*, 482, 173
- Li H., Miller J. A., 1997, *ApJ*, 478, L67
- Li H., Kusunose M., Liang E. P., 1996, *ApJ*, 460, L29
- Lubiński P., Zdziarski A. A., 2001, *MNRAS*, submitted
- McConnell M. L. et al., 1994, *ApJ*, 424, 933
- McConnell M. L. et al., 2000a, *ApJ*, 543, 928
- McConnell M. L. et al., 2000b, in McConnell M. L., Ryan J. M., eds., *AIP Conf. Proc. Vol. 510, The Fifth Compton Symposium*. Melville, New York, p. 114
- Narayan R., Yi I., 1995, *ApJ*, 452, 710
- Özel F., Psaltis D., Narayan R., 2000, *ApJ*, 541, 234
- Poutanen J., Coppi P. S., 1998, *Physica Scripta*, T77, 57
- Rybicki G. R., Lightman A. P., 1979, *Radiative Processes in Astrophysics*. Wiley-Interscience, New York
- Sunyaev R. A., Titarchuk L. G., 1980, *A&A*, 86, 121
- Treves A. et al., 1980, *ApJ*, 242, 1114
- Wardziński G., Zdziarski, A. A., 2000, *MNRAS*, 314, 183 (WZ00)
- Zdziarski A. A., 1985, *ApJ*, 289, 514
- Zdziarski A. A., 1986, *ApJ*, 303, 94
- Zdziarski, A. A. 1999, in Poutanen J., Svensson, R., eds., *ASP Conf. Ser. Vol. 161, High Energy Processes in Accreting Black Holes*. ASP, San Francisco, p. 16 (astro-ph/9812449)
- Zdziarski A. A., Poutanen J., Miłkołajewska J., Gierliński M., Ebisawa K., Johnson W. N., 1998, *MNRAS*, 301, 435
- Zdziarski A. A., Lubiński P., Smith D. A., 1999, *MNRAS*, 303, L11

This paper has been produced using the Royal Astronomical Society/Blackwell Science L<sup>A</sup>T<sub>E</sub>X style file.